ISPRS Annals of the Photogrammetry, Remote Sensing and Spatial Information Sciences, Volume XII-4/W2-2026
10th International Conference on Smart Data and Smart Cities (SDSC), 29 September–1 October 2026, Sofia, Bulgaria

A Digital Twin to Improve the Sustainability of Neighbourhood Scenario Planning

Rakibun Athid[1], Mila Koeva[1], Pirouz Nourian[1], Ulla-Britt Krämer[2]

[1] Faculty of Geo-Information Science and Earth Observation (ITC), University of Twente, Enschede, The Netherlands – r.athid@student.utwente.nl, (m.n.koeva, p.nourian)@utwente.nl
[2] Province of Overijssel, The Netherlands – UB.Kraemer@overijssel.nl

Keywords: Urban Digital Twin, Neighbourhood Sustainability, Interactive Urban Dashboards, Energy Transition Planning

Abstract

Neighbourhood sustainability planning needs tools that integrate heterogeneous urban datasets, expose modelling assumptions, and allow transparent comparison of intervention strategies across domains. Therefore, this paper presents a neighbourhood-scale urban digital twin (UDT) prototype for Twekkelerveld, Enschede, combining energy and ecological indicators in a single interactive environment. The co-developed prototype links building-level energy demand, rooftop photovoltaic potential, vegetation and tree-based ecosystem indicators, and satellite-derived urban heat information within a shared GIS-based workflow. Its main contribution is a reproducible integration pipeline that harmonises geospatial, statistical, ecological, and remote-sensing data through explicit, editable scenario-response functions. Technical validation confirmed consistent scenario behaviour. Regression-based explanatory analysis of 800 Monte Carlo runs showed that PV economic outcomes depend mainly on PV unit cost and yield assumptions, while tree annualised cost is driven by intervention cost, discounting, and time horizon. Multi-criteria decision analysis (MCDA) rankings stayed highly stable under 20% weight variation (median Spearman's $\rho \approx 0.998$), and stakeholder feedback confirmed practical usefulness for neighbourhood planning. The results show that neighbourhood-scale digital twins can support urban informatics and smart-city decision-making by making trade-offs among retrofitting, photovoltaics, greening, heat mitigation, and spatial equity visible in practice.

1. Introduction

Urban Digital Twins (UDTs) are operational digital representations of urban systems that integrate data, analytics, and simulation to support planning and decision-making (Batty, 2018; Lehtola et al., 2022). Unlike static 3D city models, a UDT is designed to help users test alternatives, compare outcomes, and connect analysis to implementation (White et al., 2021). This matters at the neighbourhood scale, where interventions interact across domains. Building retrofits affect energy demand, while trees and canopies influence both thermal comfort and solar access. In that context, UDTs provide a useful way to examine cross-domain trade-offs in a spatially explicit and evidence-based manner.

Buildings are a major source of emissions and energy demand. They account for roughly 40% of global carbon emissions (IPCC, 2022), and in the EU, they represent about 40% of final energy consumption and 36% of CO_2 emissions (European Commission, 2020). Because new construction rates are low, the existing building stock must carry much of the transition burden. This makes renovation strategies slow, capital-intensive, and dependent on inherited systems and materials (Economidou et al., 2020). At the same time, neighbourhoods are increasingly exposed to heat stress, and rising cooling demand links climate adaptation directly to decarbonisation efforts (Santamouris, 2015; Sherwood and Huber, 2010). Nature-based measures can reduce local heat exposure, but their effectiveness depends on urban form, placement, and maintenance (Bowler et al., 2010; Gunawardena et al., 2017). These choices are interconnected: the same tree canopy that cools outdoor spaces can also reduce rooftop solar access.

Building energy performance is shaped by building type, age, operation patterns, and occupant behaviour, and estimates are highly sensitive to data quality and modelling assumptions (Swan and Ugursal, 2009; Reinhart and Cerezo Davila, 2016). Reviews of urban building energy modelling (UBEM) show that reliable results depend strongly on the quality and detail of input data (Reinhart and Cerezo Davila, 2016). At the neighbourhood scale, such data are often scattered and difficult to synthesise. Planners therefore rely on proxies and simplified scenario rules. Similar constraints apply to outdoor thermal assessment. Indicators such as Physiological Equivalent Temperature (PET) depend on temperature, humidity, wind, radiation, and urban form (Höppe, 1999; Lindberg et al., 2015). Vegetation metrics, such as the Normalized Difference Vegetation Index (NDVI), tree-canopy attributes derived from light detection and ranging (LiDAR), and detailed land-cover data can reveal important benefits for cooling, stormwater management, and biodiversity (Francis et al., 2023; Konijnendijk, 2023). A rooftop solar assessment similarly requires geometric and environmental inputs, such as roof form, orientation, shading, and irradiation (Tripathy et al., 2024).

Although methods within individual domains have advanced, neighbourhood transition planning still lacks practical workflows for integrating multi-domain evidence into clear, explainable scenario choices (Lei et al., 2023). Energy and ecology analyses are often produced in separate pipelines, with different input data, units, formats, timescales, and semantics, making direct comparison difficult (Batty, 2018). Simplifications such as archetypes, defaults, proxies, and imputation are usually unavoidable, but trust declines when those assumptions are hidden or hard to trace (Swan and Ugursal, 2009; Reinhart and Cerezo Davila, 2016; Razavi et al., 2021). Technically sound tools are also not always adopted when interfaces are confusing, outputs are misaligned with planning tasks, or interpretation requires specialist expertise (Pelzer, 2017). This gap between technical capability and practical use remains a consistent barrier.

This study addresses that gap by developing a neighbourhood-scale UDT prototype in Twekkelerveld, Enschede, the Netherlands. The prototype combines several energy indicators. These include (i) baseline energy use intensity (EUI) from aggregated consumption; (ii) retrofit savings of up to 25%, parameterised by construction year; (iii) photovoltaic (PV) generation from rooftop irradiation rasters that account for shading and orientation; and (iv) operational carbon dioxide (CO_2) emissions based on carrier-specific emission factors. It also includes ecological indicators such as (1) NDVI from Landsat-9 red and near-infrared (NIR) bands, (2) land-surface-temperature-based urban heat island (UHI) intensity relative to a rural baseline, (3) tree cooling effects of about 1 to 3 °C with distance decay, (4) stormwater retention through canopy interception factors, and (5) corridor connectivity derived from gap-threshold analysis. Heterogeneous data sources, including Basisregistratie Adressen en Gebouwen (BAG) building footprints, aggregated gas and electricity consumption, Landsat-9 imagery, municipal tree inventories, Basisregistratie Grootschalige Topografie (BGT) green polygons, and Actueel Hoogtebestand Nederland (AHN) LiDAR elevation, were harmonised into a shared spatial framework using European Petroleum Survey Group (EPSG) 4326 for web delivery and EPSG 28992 (Amersfoort / RD New) for metric analysis (Open Geospatial Consortium, 2021; Open Geospatial Consortium, 2023).

The co-developed CesiumJS-based prototype allows users to create and compare intervention packages using sliders for retrofit, PV, and tree planting on a 0–100% scale. It also includes geospatial drawing tools for ecological interventions, such as trees, green facades, and green roofs, each linked to explicit benefit coefficients. In addition, it includes a multi-criteria decision analysis (MCDA) interface that ranks options under stated budget constraints using a weighted-sum model applied to normalised criteria. Scenario logic is implemented through explicit scenario-response functions in which indicator changes are computed as $I(s) = I_0 + A \cdot u(s)$, where I_0 represents the baseline indicator vector, $u(s)$ the intervention-intensity vector, and A is a matrix of editable effect coefficients. Testing confirmed the expected monotonic responses, MCDA rankings that stayed stable under $\pm 20\%$ weight variation, and stakeholder agreement of 84% to 98% across the seven prototype components (Sections 3.5 and 3.6).

In this context, this study addresses two questions. First, how can neighbourhood-scale UDTs combine energy and ecological indicators in a transparent, interactive workflow that supports evidence-based planning? Second, how do small, spatially targeted interventions affect the combined sustainability indicator set, including cross-domain synergies and trade-offs between indicators?

This paper makes three main contributions. First, it presents a neighbourhood-scale urban digital twin that integrates heterogeneous datasets on energy, ecology, statistics, and remote sensing into a common spatial framework for local sustainability planning. Second, it implements a transparent scenario-planning workflow based on explicit, editable scenario-response functions and a web-based 3D interface with MCDA support. Third, it evaluates the prototype through technical validation and stakeholder review to assess its usefulness as a practical planning support tool. The work sits within geographic information systems (GIS), urban informatics, smart-city ICT, city analytics, open urban data workflows, and interactive urban dashboards, transforming fragmented urban data into actionable scenario information for neighbourhood-scale decision-making.

2. Materials and Methods

2.1 Study Area

Twekkelerveld, a post-war residential neighbourhood in Enschede, the Netherlands, was selected because it is representative of the Dutch 1950s–1960s housing stock that now needs both retrofitting and climate adaptation. The neighbourhood has a relatively dense residential layout, limited canopy cover, and fragmented green spaces, which makes it a practical test case for integrated neighbourhood-scale interventions (Figure 1).

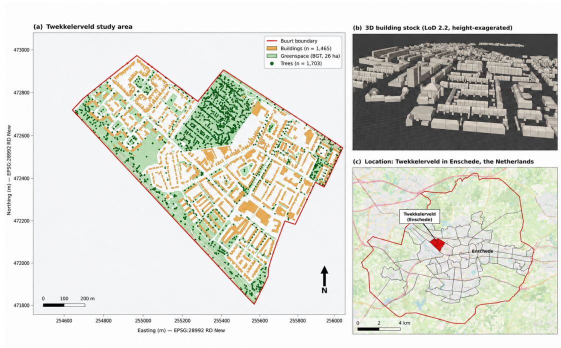

Figure 1. Study area of Twekkelerveld, Enschede: (a) buildings, greenspace, and trees within the neighbourhood (buurt) boundary; (b) 3D building stock at LoD 2.2; (c) location within Enschede, the Netherlands. Metric coordinates in EPSG:28992 (Amersfoort / RD New). Source: authors, based on BAG, BGT, AHN, 3DBAG, and OpenStreetMap data.

2.2 Dataset description

Table 1 lists the core datasets used in the prototype, their role in the analysis, and their sources.

2.3 Preprocessing and Harmonisation

All source datasets (Table 1) were harmonised for spatial and semantic consistency and interoperability, following Open Geospatial Consortium (OGC) encodings for geospatial data (Open Geospatial Consortium, 2021; Open Geospatial Consortium, 2023). Harmonisation was organised in three stages that correspond to the pre-processing block in Figure 2: spatial standardisation, attribute harmonisation, and quality assurance. Spatial standardisation established a common geometric frame. The Twekkelerveld boundary polygon was extracted from OpenStreetMap via an Overpass API query, checked against official municipal boundaries, and used as the clipping mask for all other layers. For metric operations, such as area measurement, buffering, and Euclidean distance calculation, source data were reprojected to EPSG 28992 (Amersfoort / RD New), the Dutch national grid. For web delivery and 3D visualisation, outputs were exported to EPSG 4326 to align with CesiumJS and the Web Graphics Library (WebGL). Coordinate reference metadata were checked across all sources to reduce systematic spatial misalignment, a common issue in multi-source urban geospatial workflows (Nourian et al., 2018); raster layers

Dataset/source	Main use in this study	Reference
BAG and BGT building footprints; VBO attributes	Geometry, identifiers, floor area, land use	(PDOK, 2023b; PDOK, 2023c)
AHN4 DSM/DTM and 3DBAG LoD2.2	Elevation, roof structure, shading, 3D view	(PDOK, 2023a; Peters et al., 2022)
CBS residential gas and electricity statistics	Neighbourhood energy baseline	(CBS, 2022)
BGT greenspace polygons and municipal tree inventory	Greenspace and tree structure analysis	(PDOK, 2023c)
DSM-derived tree objects	Tree-canopy extraction and validation	This study
Landsat-9 Collection 2 Level 2 (7 Aug 2022; <5% cloud)	NDVI, surface temperature, UHI proxy	(USGS, 2022)

Table 1. Core datasets used in the Twekkelerveld neighbourhood digital twin

were kept on their shared 30 m Landsat grid, then reprojected and clipped to the neighbourhood boundary to align with the vector layers. Attribute harmonisation brought the heterogeneous source schemas onto a single building and grid-referenced data model. Field names and identifiers were standardised across the building registers: BAG pand (building) identifiers were normalised by stripping namespace prefixes (for example, NL.IMBAG.Pand.), and the BAG footprints, VBO (Verblijfsobject) residential-unit records, and the aggregated energy statistics were keyed to a common building identifier, with null values retained for unmatched records rather than silently dropped. This register chain matched 97.3% of buildings (1,425 of 1,465). Units were harmonised to kWh/m^2/year, m^2, tCO_2/year, and °C. The two tree sources, an open-data canopy layer derived from BGT vegetation and AHN heights and the municipal tree inventory, were cross-checked rather than blindly merged. Quality assurance then validated geometric and attribute completeness, flagged missing values and outliers, and documented the residual data gaps.

The harmonised dataset was produced offline and packaged into open, web-ready formats rather than being uploaded wholesale to a hosting service. The pipeline is implemented in QGIS 3.40.1 and Python (geopandas, rasterio, shapely, and pyproj) and exports three standard encodings: GeoJSON for vector features, Cloud-Optimised GeoTIFF for raster surfaces, and OGC 3D Tiles for the building meshes, the last reconstructed from 3DBAG LoD 2.2 CityJSON and prepared in Blender. These static assets are read directly by the browser client; only the 3D visualisation mesh is hosted through a Cesium ion tileset, while all indicator, scenario, and MCDA computation runs client-side without a server-side spatial database or geoprocessing backend. Keeping the harmonised data as portable, standard files means the layers remain inspectable and a municipality can host the prototype on its own infrastructure. The operational integration pipeline is summarised in Figure 2, which traces the workflow from raw inputs and preprocessing through cross-domain fusion to outputs and validation.

2.4 Indicator Modelling and Scenario Logic

Indicator modelling used a set of planning-oriented energy and ecological indicators that could be updated, compared, and combined within a shared scenario environment. The approach deliberately prioritised transparency and cross-domain integration over high-fidelity simulation: the indicators are planning proxies rather than exhaustive process models, and keeping proxies, defaults, and effect coefficients visible and editable was treated as a first-class requirement that was itself evaluated in the stakeholder review (Section 3.6). Building en-

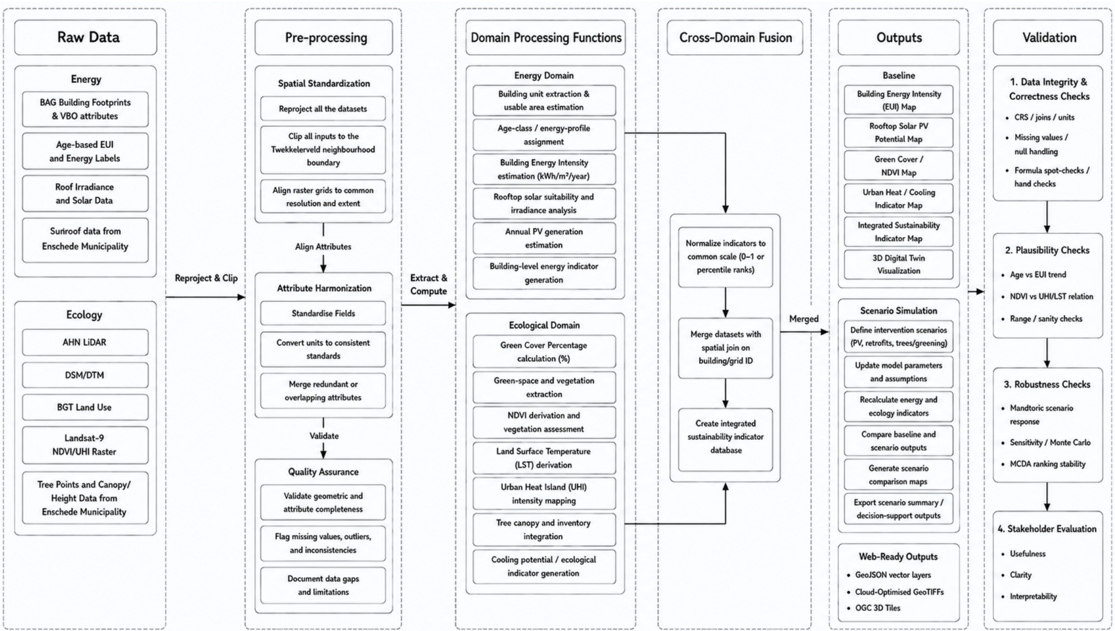

Figure 2. Methodological workflow.

ergy indicators were derived through a multi-step join: Verblijfsobject (residential-unit) records were spatially joined to pand footprints and aggregated by usable floor area, and buildings without a valid link were assigned a default area of twice the footprint (two storeys), validated against regional building-stock typologies (Itard et al., 2008). Energy use intensity (EUI, kWh/m^2/year) was the ratio of annual energy to usable floor area, and buildings were split into low-, medium-, and high-EUI tertiles (P33, P66). Rooftop photovoltaic (PV) potential was estimated in two stages: pixel-based solar irradiance accounting for orientation, slope, and obstructions, and suitability analysis of viable roof segments. Irradiance was modelled with the SEBE method in the UMEP plugin (Lindberg et al., 2018), summing direct, diffuse, and reflected components (Lindberg et al., 2015) over a Typical Meteorological Year for Enschede (EU-JRC, 2026), with shadows from an AHN-derived DSM. PV generation used monocrystalline-silicon efficiency (η = 18%), a performance ratio of 0.85, and temperature derating (Mayer et al., 2020).

Tree ecosystem services were quantified with a hybrid approach combining open-data analysis, inventory attributes, and municipal tree records used to validate species and size. Carbon sequestration used species-specific growth models (Nowak and Crane, 2002), with annual CO_2 uptake of 10–30 kg/tree/year. Cooling effects were parameterised from urban-climate meta-analyses (typically 1–3 °C within 50 m of tree clusters, attenuating with distance; (Bowler et al., 2010; Gunawardena et al., 2017)). Stormwater interception used canopy interception coefficients (0.15–0.25 of precipitation) applied to local Royal Netherlands Meteorological Institute (KNMI) precipitation records (Xiao and McPherson, 2002; Royal Netherlands Meteorological Institute, 2022). Green corridor connectivity was assessed using gap-threshold analysis, where green-space patches separated by more than 150 m were treated as disconnected (Gren et al., 2009).

$$\begin{aligned} I(s) &= I_0 + A \cdot u(s) && (1) \\ \text{NDVI} &= (\text{NIR} - \text{Red})/(\text{NIR} + \text{Red}) && (2) \\ \text{Score}(s) &= \sum_j w_j z_j(s), \quad \text{with} \quad \sum_j w_j = 1 && (3) \end{aligned}$$

where $I(s)$ is the scenario indicator vector, I_0 the baseline indicator vector, $u(s)$ the intervention-intensity vector, A the editable effect-coefficient matrix, NDVI the normalised difference vegetation index, NIR and Red the near-infrared and red bands, $z_j(s)$ the normalised score of criterion j under scenario s, and w_j the weight of criterion j.

3. Results

3.1 Digital Twin Prototype Architecture and Functionality

The DT prototype is a modular, web-based environment linking an overview landing page with dedicated ecology, energy, and combined scenario-analysis workspaces (Figures 3–6). This structure follows the workflow in Figure 2: harmonised spatial layers feed indicator calculations, those indicators appear through map-based views and dashboards, and user-defined interventions update scenario outputs in real time.

Together, Figures 3 to 6 keep baseline diagnostics, domain-specific interventions, and integrated scenario comparison visually distinct but analytically connected.

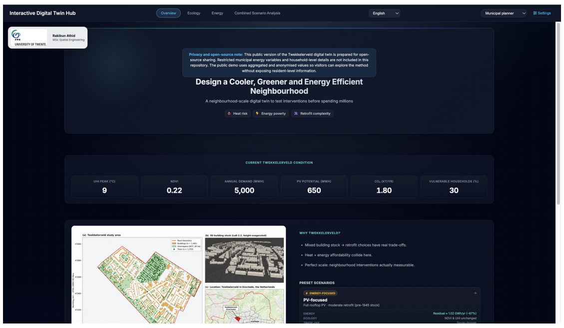

Figure 3. Interactive overview and baseline headline indicators.

3.2 Baseline Energy Performance

Baseline energy results show a clear age gradient in the Twekkelerveld building stock (Table 2; Figure 4). Median Energy Use Intensity (EUI) is highest in the pre-1970 stock and declines steadily across newer construction cohorts, confirming that retrofit need is concentrated in the oldest residential buildings.

Construction period	N	Median EUI (kWh/m^2/yr)
Pre-1970	1,142	168.2
1970-1990	79	153.6
1990-2010	148	131.6
Post-2010	96	117.0

Table 2. Median EUI by construction period in Twekkelerveld (**N** = number of buildings in each construction-period group)

Within the pre-1970 cohort, the pre-1945 subgroup records the highest median demand at 182.8 kWh/m^2/year, and 244 buildings (16.7% of the dataset) exceed 180 kWh/m^2/year, indicating high-EUI cases. At the neighbourhood scale, total annual demand is about 39.3 GWh, of which 31.3 GWh comes from gas and 8.0 GWh from electricity; residential buildings account for about 89.8% of total demand. Building-level PV attributes also reveal clear spatial variation in roof suitability and expected output, allowing relative comparison of installation opportunities across the neighbourhood, although these values should be interpreted as technical screening estimates rather than bankable production forecasts.

Figure 4. Energy module interface.

3.3 Baseline Ecology and Heat Performance

The ecology baseline shows two linked conditions: limited greenness and fragmented cooling capacity (Figure 5). Across

912 valid Landsat-9 pixels, NDVI ranges from 0.06 to 0.40 with a median of 0.19, and only 9.2% of pixels exceed 0.30. Denser vegetation is confined to small pockets rather than forming a continuous neighbourhood cooling network.

Tree datasets reinforce this interpretation. The DSM-derived layer identifies 1,703 canopy or tree objects, whereas the municipal inventory lists 2,451 records, because the inventory also contains younger or closely spaced trees that are not always separable in the open-data canopy extraction. Median tree height is 8.9 m and median crown area is 47.1 m^2, suggesting a relatively mature but unevenly distributed urban tree stock.

Thermal patterns follow the expected vegetation gradient. Land surface temperature on 7 August 2022 ranges from 29.0 °C to 40.4 °C with a median of 35.2 °C, and pixels with NDVI $\geq$ 0.30 are 4.9 °C cooler at the median than pixels with NDVI $<$ 0.10. The negative NDVI–UHI relationship (Spearman's $\rho = -0.448$, $p < 0.001$) is consistent with cooler surface conditions in greener areas, although this association should not be interpreted as a causal estimate of intervention effect. The fragmented greenspace structure nevertheless limits neighbourhood-wide continuity: only three connected networks larger than 0.5 ha were identified, and 44% of households lie beyond 300 m walking distance from the main connected patch. In practical terms, the baseline ecology results point to a need for strategically placed greening rather than uniformly distributed, low-intensity additions.

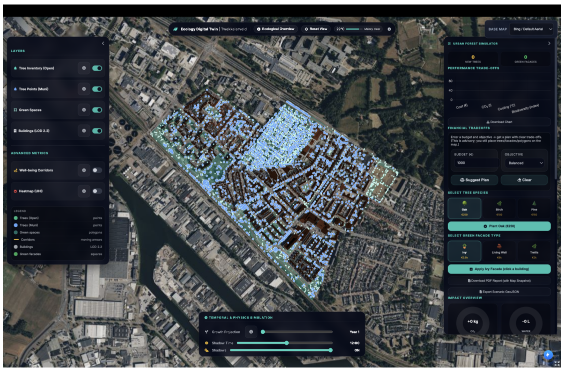

Figure 5. Ecology module interface.

3.4 Scenario Analysis and Intervention Comparison

Using the combined dashboard shown in Figure 6, three illustrative scenarios were tested in the prototype to examine cross-domain trade-offs: S1 was energy focused (+50% rooftop PV and 30% insulated buildings), S2 was ecology focused (500 additional trees and 20% green-roof coverage), and S3 combined both domains (300 additional trees, +30% rooftop PV, 20% insulated buildings, and 10% green-roof coverage). Because these results were generated by the embedded client-side scenario engine, they should be interpreted as prototype-based comparative estimates rather than fully calibrated forecasts for the neighbourhood.

In S1, annual energy demand fell from 5.0 GWh to 4.48 GWh (−10.4%), while PV generation rose from 0.65 to 0.98 GWh/year. Net grid demand therefore dropped from 4.35 to 3.50 GWh/year (−19.5%), and operational emissions decreased from 1,800 to 1,612 tCO_2/year. Since S1 did not include greening, NDVI remained at 0.22, and the mean UHI changed only slightly, to 8.41 °C. In S2, ecological indicators improved substantially: mean NDVI increased from 0.22 to 0.248 and mean UHI decreased from 9.0 to 8.63 °C. Annual energy demand decreased only marginally to 4.86 GWh because the current model captures only limited cooling co-benefits, and the built-in tree-shading penalty reduced PV generation from 0.65 to 0.54 GWh/year. S3 produced the most balanced outcome: mean NDVI increased to 0.236, mean UHI decreased to 8.43 °C, annual energy demand declined to 4.59 GWh (−8.2%), and PV generation increased to 0.76 GWh/year.

Across all tested scenarios, the prototype behaved as expected: increasing PV settings raised solar output, stronger retrofit settings lowered energy demand, and additional trees improved greenness and thermal indicators. This aligns with established findings that retrofits and distributed PV reduce operational emissions, while urban greening improves local thermal conditions but can introduce shading trade-offs for rooftop solar.

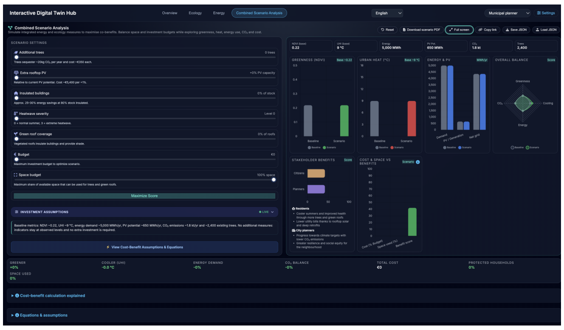

Figure 6. Combined scenario-analysis dashboard.

3.5 Technical Validation

Technical validation was designed as a six-step approach rather than a single-metric exercise. First, data-integrity checks verified that the core spatial layers used a consistent EPSG:4326 reference system and that the integrated 1,465-building BAG layer preserved a one-to-one bag_id structure with 0 duplicate keys and no missing identifiers. This check concerns the identifier itself: the 2.7% of buildings without a matched energy record (Section 2.3) still carry valid identifiers. Second, formula spot checks on five representative buildings spanning older, newer, and near-green cases reproduced annual savings exactly and kept payback error within 0.43%, confirming that the front-end energy formulas match the documented calculations.

Third, construct-plausibility checks confirmed that the integrated indicators still behaved as expected after data fusion. The age-EUI gradient remained logical, and the NDVI-UHI association across 912 pixels was negative, consistent with the expected cooling effect of vegetation. Fourth, robustness was tested through monotonicity checks, Monte Carlo sensitivity analysis, and MCDA perturbation tests. The sensitivity analysis was implemented as repeated random sampling of selected economic and ecological inputs within predefined bounds rather than as a full factorial design. All seven monotonic scenario metrics showed zero violations, 800 runs quantified uncertainty in economic and ecological outputs, and 500 weight perturbations, each followed by weight-vector renormalisation, produced a median rank correlation of 0.998, with four alternatives always remaining in the top 10 and six appearing in at least 80% of runs.

Fifth, diagnostic review assessed whether the Monte Carlo-derived relationships suited explanatory interpretation.

Residuals-versus-fitted and Q–Q plots for the final tree and PV models (Figure 7) showed residuals centred around zero with some tail deviation, but no severe non-linearity that would invalidate their use for explanatory screening. Sixth, regression-based explanatory analysis was performed on the 800 Monte Carlo runs to identify which uncertain inputs most strongly explained selected outcome indicators. The final PV model for NPV_PV explained 97.7% of the variance (adjusted R^2 = 0.977) and showed that PV unit cost was the dominant negative driver, while PV yield was the dominant positive driver. The final tree model for EAC_Trees explained 97.4% of the variance (adjusted R^2 = 0.974) and showed that the annualised tree-intervention cost was mainly driven by intervention cost per square metre, discounting, and time horizon.

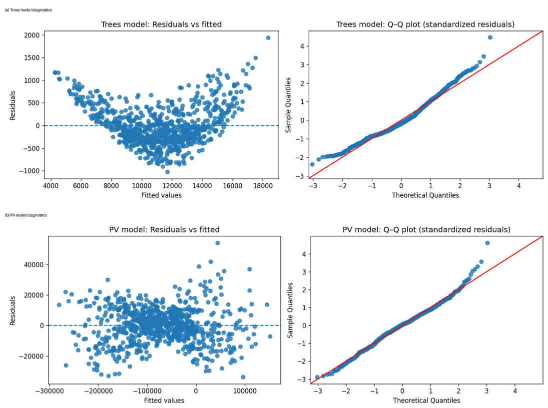

Figure 7. Residual-versus-fitted and Q–Q diagnostics for the final tree and PV regression models.

These six checks show that the prototype is internally consistent, empirically plausible, and stable enough for comparative scenario screening. The sensitivity and regression results also reveal where caution is needed: PV net present value (NPV) is driven mainly by PV unit cost and yield assumptions; insulation NPV is almost entirely determined by insulation cost per square metre; and ecological cost outputs depend strongly on intervention cost, horizon, and discounting. The digital twin should therefore be used to compare options, expose trade-offs, and support stakeholder discussion, rather than to replace project-level engineering design or procurement calculations.

3.6 Stakeholder Evaluation

Stakeholder evaluation assessed whether the prototype's outputs and interface were understandable and useful for practical planning tasks, following the planning-support usefulness framework (Pelzer, 2017) and the ISO 9241-11 usability standard. The prototype was demonstrated to 66 participants across four guided sessions: the municipalities of Enschede (20) and Hengelo (14) and the FutureBEEIng Dutch (20) and German (12) partner pools, using five-point Likert scales on the usefulness, clarity, and interpretability of seven prototype components. Agreement (Agree plus Strongly agree) lay between 84% and 98% across all components and groups, with no negative responses; the cross-domain trade-off view (97–98%) and the two domain modules (91–97%) scored highest, while the MCDA weighting step (84–88%) drew requests for clearer weight reasoning. These ratings capture perceived usefulness in a guided demonstration rather than evidence of improved planning outcomes over time.

4. Discussion

The Twekkelerveld prototype shows that energy and ecological evidence can be combined in a single neighbourhood-scale planning environment without hiding the assumptions that connect them. Its main contribution is not a single indicator or visualisation. Rather, it is the transparent integration workflow. This workflow harmonises heterogeneous datasets, links them through explicit scenario-response functions, and presents them in an interactive dashboard. The digital twin works as both a planning support tool and a neighbourhood-scale urban analytics environment.

The energy results are more useful for prioritisation than for exact forecasting. The age pattern in energy performance suggests that retrofit need is concentrated in older parts of the housing stock, consistent with the historical evolution of Dutch building standards (Itard et al., 2008). The prototype can therefore help identify where bundled retrofit programmes may be most effective. That said, technical priority should not automatically translate into social priority. Affordability, seasonality, and vulnerability matter when moving from screening to implementation (Bouzarovski and Petrova, 2015). The rooftop PV results also indicate a relative technical opportunity. However, they should still be interpreted as screening-level estimates, because actual deployment will depend on ownership, grid capacity, and investment conditions.

The ecological findings point to a second structural issue. Limited greenness is accompanied by a fragmented cooling network. The observed NDVI–UHI pattern is useful because it shows that greener parts of the neighbourhood were cooler in the analysed summer scene. This is consistent with earlier urban heat studies (Bowler et al., 2010; Gunawardena et al., 2017). At the same time, this relationship should not be interpreted as a causal estimate of intervention impact. In this study, the empirical association is derived from a single Landsat observation. It therefore serves mainly as supporting evidence for comparative scenario design, rather than as proof of how much cooling a specific intervention will cause.

A regression-based explanatory analysis of 800 Monte Carlo runs was added for selected intervention outputs, which strengthens the interpretation of the uncertainty results but does not resolve causal attribution for local thermal effects. Combining DSM-based tree detection with the municipal inventory nevertheless strengthens the comparative analysis by showing where vegetation is present, how it is distributed, and where additional greening may plausibly improve connectivity and heat mitigation. The findings are therefore more robust for comparing alternatives than for making precise causal or compliance claims, including against frameworks such as 3-30-300 (Konijnendijk, 2023).

The scenario comparisons show why integrated planning matters. Energy-oriented measures produced stronger near-term mitigation gains. Greening-oriented measures produced clearer adaptation benefits, but weaker direct mitigation effects. The value of the prototype lies in making these trade-offs visible within one shared interface rather than treating the domains separately. This matters because neighbourhood planning rarely involves a single objective. In practice, it requires balancing emissions, heat exposure, ecosystem services, spatial access, and budget constraints at the same time (IPCC, 2022; Ramaswami et al., 2016). The platform should therefore be understood as a deliberative tool for exploring combined pathways, not as an automated optimiser that determines one objectively best solution.

The validation and regression results should also be interpreted carefully. They indicate internal consistency, comparative robustness, and structured model behaviour, not full predictive accuracy. The monotonicity checks, formula spot checks, random-sensitivity runs, regression analysis, and MCDA-weight perturbations addressed related but distinct questions: whether the engine responded in the expected direction, whether outputs reproduced the documented calculations, whether the ranking structure remained stable when uncertain inputs and preferences were varied within plausible bounds, and which assumptions most strongly explained variation in key outcomes. This is important because the MCDA combines incommensurate criteria by first normalising them to a common unitless scale and then applying a weighted-sum model (Malczewski and Rinner, 2015). That approach is suitable for transparent screening. However, it also means that rankings depend partly on the chosen normalization method and on stakeholder weights. Likewise, the regression results describe model-based relationships within the simulated uncertainty space, not direct causal effects in the real neighbourhood. For that reason, the outputs should support discussion and justification, not replace expert judgement.

This study has several limitations. Landsat thermal data at 100 m resolution can detect neighbourhood-scale patterns, but are too coarse for street-level microclimate analysis. The single-date image also fails to capture seasonal variation. Energy estimates are based on aggregated annual consumption due to General Data Protection Regulation (GDPR) constraints, so they do not capture peak loads or occupancy dynamics. PV generation is modelled under standard assumptions, excluding soiling, degradation, and year-to-year climate variability, all of which may reduce long-term yield by roughly 10–15% (Jordan and Kurtz, 2013). The literature on tree ecosystem services uses generic rates rather than local species-specific models. Cooling effects are parameterised from meta-analyses, not local field measurements or causal ecological regression. The regression analysis is based on simulated Monte Carlo outputs rather than observed data and should be read as model-based explanatory analysis within the defined uncertainty space. The MCDA weighted-sum model assumes preferential independence and linear value functions, which may not hold for complex urban objectives that involve thresholds and non-linear responses (Malczewski and Rinner, 2015). Future work should extend temporal dynamics, strengthen calibration, and refine usability while preserving the transparency of the current planning-support workflow.

5. Conclusion

This paper presented a neighbourhood-scale urban digital twin integrating heterogeneous energy, ecological, remote-sensing, and 3D spatial datasets into a transparent scenario-planning workflow for local sustainability planning. The prototype showed that explicit scenario-response functions, web-based interactive visualisation, and MCDA support help users explore cross-domain trade-offs between retrofit, photovoltaics, greening, heat mitigation, and spatial equity within a single neighbourhood-scale environment. Its value is not in high-fidelity prediction but in making assumptions inspectable, comparisons reproducible, and intervention choices easier to discuss. The regression-based explanatory analysis further showed that PV outcomes are most sensitive to PV cost and yield assumptions, while annualised tree-intervention cost depends mainly on intervention cost, discounting, and time horizon. Future work should improve temporal dynamics, strengthen domain calibration, and refine usability for less technical users, while maintaining transparency and interoperability that make the prototype a practical smart-city decision-support tool.

Acknowledgements

This research was carried out within FutureBEEIng, an Interreg A (Netherlands/Germany) programme coordinated by the Province of Overijssel. The authors thank the programme partners and the municipalities of Enschede and Hengelo for the case context and the stakeholder evaluation reported in Section 3.6. The authors also thank Bram Reinders, Stéphanie Reinders, and Yashar Hajimolana from Twinlink.eu for their willingness to further develop the work for other municipalities.

References

Batty, M., 2018. Digital twins. *Environ. Plan. B Urban Anal. City Sci.*, 45(5), 817–820. doi.org/10.1177/2399808318796416.

Bouzarovski, S., Petrova, S., 2015. A global perspective on domestic energy deprivation: Overcoming the energy poverty–fuel poverty binary. *Energy Res. Soc. Sci.*, 10, 31–40. doi.org/10.1016/j.erss.2015.06.007.

Bowler, D. E., Buyung-Ali, L., Knight, T. M., Pullin, A. S., 2010. Urban greening to cool towns and cities: A systematic review of the empirical evidence. *Landscape Urban Plann.*, 97(3), 147–155. doi.org/10.1016/j.landurbplan.2010.05.006.

CBS, 2022. Kerncijfers wijken en buurten 2022 [Key figures for neighbourhoods 2022]. Statistics Netherlands. opendata.cbs.nl/statline/ (10 March 2026).

Economidou, M., Todeschi, V., Bertoldi, P., D'Agostino, D., Zangheri, P., Castellazzi, L., 2020. Review of 50 years of EU energy efficiency policies for buildings. *Energy Build.*, 225, 110322. doi.org/10.1016/j.enbuild.2020.110322.

EU-JRC, 2026. PVGIS User Manual (PVGIS 5.3). European Commission, Joint Research Centre. joint-research-centre.ec.europa.eu/photovoltaic-geographical-information-system-pvgis/getting-started-pvgis/pvgis-user-manual_en (18 March 2026).

European Commission, 2020. Energy efficiency in buildings – EU statistics. Eurostat catalogue no E2020. ec.europa.eu/eurostat/web/energy/data/database (12 March 2026).

Francis, J., Disney, M., Law, S., 2023. Monitoring canopy quality and improving equitable outcomes of urban tree planting using LiDAR and machine learning. *Urban For. Urban Green.*, 89, 128115. doi.org/10.1016/j.ufug.2023.128115.

Gren, Å., Andersson, E., Söderman, T., 2009. Landscape fragmentation and connectivity: Quantification and ecological assessment of greenspace structure. M. J. McDonnell, A. K. Hahs, J. H. Breuste (eds), *Ecology of cities and towns: A comparative approach*, Cambridge University Press, Cambridge, 183–201.

Gunawardena, K. R., Wells, M. J., Kershaw, T., 2017. Utilising green and bluespace to mitigate urban heat island intensity. *Sci. Total Environ.*, 584–585, 1040–1055. doi.org/10.1016/j.scitotenv.2017.01.158.

https://doi.org/10.5194/isprs-annals-XII-4-W2-2026-17-2026

Höppe, P., 1999. The physiological equivalent temperature—A universal index for the biometeorological assessment of the thermal environment. *Int. J. Biometeorol.*, 43(2), 71–75. doi.org/10.1007/s004840050118.

IPCC, 2022. *Climate change 2022: Mitigation of climate change. Contribution of Working Group III to the Sixth Assessment Report of the Intergovernmental Panel on Climate Change*. Cambridge University Press, Cambridge. Shukla, P. R., Skea, J., Slade, R., Al Khourdajie, A., van Diemen, R., McCollum, D., Pathak, M., Some, S., Vyas, P., Fradera, R., Belkacemi, M., Hasija, A., Lisboa, G., Luz, S., Malley, J. (Eds.).

Itard, L., Meijer, F., Vrins, E., Hoiting, H., 2008. Building renovation and modernisation in Europe: State of the art review. Technical report, OTB Research Institute for Housing, Urban and Mobility Studies, Delft University of Technology, Delft.

Jordan, D. C., Kurtz, S. R., 2013. Photovoltaic degradation rates—An analytical review. *Prog. Photovolt. Res. Appl.*, 21(1), 12–29. doi.org/10.1002/pip.1182.

Konijnendijk, C. C., 2023. Evidence-based guidelines for greener, healthier, more resilient neighbourhoods: Introducing the 3-30-300 rule. *J. For. Res.*, 34(4), 821–830. doi.org/10.1007/s11676-022-01523-z.

Lehtola, V. V., Koeva, M., Elberink, S. O., Raposo, P., Virtanen, J.-P., Vahdatikhaki, F., Borsci, S., 2022. Digital twin of a city: Review of technology serving city needs. *Int. J. Appl. Earth Obs. Geoinf.*, 114, 102915. doi.org/10.1016/j.jag.2022.102915.

Lei, B., Stouffs, R., Biljecki, F., Cai, H., 2023. Challenges of urban digital twins: A systematic review and a Delphi expert survey. *Autom. Constr.*, 147, 104716. doi.org/10.1016/j.autcon.2022.104716.

Lindberg, F., Grimmond, C. S. B., Gabey, A., Huang, B., Kent, C. W., Sun, T., Theeuwes, N. E., Järvi, L., Ward, H. C., Capel-Timms, I., Chang, Y., Jonsson, P., Krave, N., Liu, D., Meyer, D., Olofson, K. F. G., Tan, J., Wästberg, D., Xue, L., Zhang, Z., 2018. Urban Multi-scale Environmental Predictor (UMEP): An integrated tool for city-based climate services. *Environ. Model. Softw.*, 99, 70–87. doi.org/10.1016/j.envsoft.2017.09.020.

Lindberg, F., Jonsson, P., Honjo, T., Wästberg, D., 2015. Solar energy on building envelopes-3D modelling in a 2D environment. *Sol. Energy*, 115, 369–378. doi.org/10.1016/j.solener.2015.03.001.

Malczewski, J., Rinner, C., 2015. *Multicriteria decision analysis in geographic information science*. Springer, Berlin.

Mayer, M. J., Szilágyi, A., Gróf, G., 2020. Environmental and economic multi-objective optimization of a household level hybrid renewable energy system by genetic algorithm. *Appl. Energy*, 269, 115058. doi.org/10.1016/j.apenergy.2020.115058.

Nourian, P., Martinez-Ortiz, C., Ohori, K. A., 2018. Essential means for urban computing: Specification of web-based computing platforms for urban planning, a hitchhiker's guide. *Urban Planning*, 3(1), 21–41. doi.org/10.17645/up.v3i1.1299.

Nowak, D. J., Crane, D. E., 2002. Carbon storage and sequestration by urban trees in the USA. *Environ. Pollut.*, 116(3), 381–389. doi.org/10.1016/S0269-7491(01)00214-7.

Open Geospatial Consortium, 2021. OGC City Geography Markup Language (CityGML) 3.0 Conceptual Model. Kolbe, T. H., Nagel, C., Becker, T. (Eds.). opengis.net/doc/IS/CityGML-1/3.0 (5 March 2026).

Open Geospatial Consortium, 2023. OGC CityJSON Community Standard 2.0. docs.ogc.org/cs/20-072r2/20-072r2.html (8 March 2026).

PDOK, 2023a. Actueel Hoogtebestand Nederland (AHN). Publieke Dienstverlening Op de Kaart. pdok.nl/introductie/-/article/actueel-hoogtebestand-nederland-ahn (20 March 2026).

PDOK, 2023b. Basisregistratie Adressen en Gebouwen (BAG). Publieke Dienstverlening Op de Kaart. pdok.nl/introductie/-/article/basisregistratie-adressen-en-gebouwen-ba-1 (20 March 2026).

PDOK, 2023c. Basisregistratie Grootschalige Topografie (BGT). Publieke Dienstverlening Op de Kaart. pdok.nl/introductie/-/article/basisregistratie-grootschalige-topografie (20 March 2026).

Pelzer, P., 2017. Usefulness of planning support systems: A conceptual framework and an empirical illustration. *Transp. Res. Part A Policy Pract.*, 104, 84–95. doi.org/10.1016/j.tra.2016.06.019.

Peters, R., Dukai, B., Vitalis, S., van Liempt, J., Stoter, J., 2022. Automated 3D reconstruction of LoD2 and LoD1 models for all 10 million buildings of the Netherlands. *Photogramm. Eng. Remote Sens.*, 88(3), 165–170. doi.org/10.14358/PERS.21-00032R2.

Ramaswami, A., Russell, A. G., Culligan, P. J., Sharma, K. R., Kumar, E., 2016. Meta-principles for developing smart, sustainable, and healthy cities. *Science*, 352(6288), 940–943. doi.org/10.1126/science.aaf7160.

Razavi, S., Jakeman, A., Saltelli, A., Prieur, C., Iooss, B., Borgonovo, E., Plischke, E., Lo Piano, S., Iwanaga, T., Becker, W., Tarantola, S., Guillaume, J. H. A., Jakeman, J., Gupta, H., Melillo, N., Rabitti, G., Chabridon, V., Duan, Q., Sun, X., Maier, H. R., 2021. The future of sensitivity analysis: An essential discipline for systems modeling and policy support. *Environ. Model. Softw.*, 137, 104954. doi.org/10.1016/j.envsoft.2020.104954.

Reinhart, C. F., Cerezo Davila, C., 2016. Urban building energy modeling—A review of a nascent field. *Build. Environ.*, 97, 196–202. doi.org/10.1016/j.buildenv.2015.12.001.

Royal Netherlands Meteorological Institute, 2022. KNMI klimaatsignaal'21: Klimaatverandering in Nederland [KNMI climate signal'21: Climate change in the Netherlands]. Koninklijk Nederlands Meteorologisch Instituut. knmi.nl/kennis-en-datacentrum/achtergrond/knmi-klimaatsignaal-21 (25 March 2026).

Santamouris, M., 2015. Analyzing the heat island magnitude and characteristics in one hundred Asian and Australian cities and regions. *Sci. Total Environ.*, 512–513, 582–598. doi.org/10.1016/j.scitotenv.2015.01.060.

Sherwood, S. C., Huber, M., 2010. An adaptability limit to climate change due to heat stress. *Proc. Natl. Acad. Sci. U.S.A.*, 107(21), 9552–9555. doi.org/10.1073/pnas.0913352107.

Swan, L. G., Ugursal, V. I., 2009. Modeling of end-use energy consumption in the residential sector: A review of modeling techniques. *Renew. Sustain. Energy Rev.*, 13(8), 1819–1835. doi.org/10.1016/j.rser.2008.09.033.

Tripathy, A., Koeva, M. N., Cardenas Leon, I. L., Nourian, P., 2024. Planning support system development for analysing environmental performance of form-based design decisions: Case study of Enschede. *Int. Arch. Photogramm. Remote Sens. Spatial Inf. Sci.*, XLVIII-4/W11-2024, 137–144. doi.org/10.5194/isprs-archives-XLVIII-4-W11-2024-137-2024.

USGS, 2022. Landsat Collection 2 Level-2 Science Products. U.S. Geological Survey. usgs.gov/landsat-missions/landsat-collection-2-level-2-science-products (22 March 2026).

White, G., Zink, A., Codecá, L., Clarke, S., 2021. A digital twin smart city for citizen feedback. *Cities*, 110, 103064. doi.org/10.1016/j.cities.2020.103064.

Xiao, Q., McPherson, E. G., 2002. Rainfall interception by Santa Monica's municipal urban forest. *Urban Ecosyst.*, 6(4), 291–302. doi.org/10.1023/B:UECO.0000004828.05143.67.